

On the Relation between Particle Morphology, Structure of the Metal-Support Interface, and Catalytic Properties of Pt/ γ -Al₂O₃

Marius Vaarkamp,^{*,1} Jeffrey T. Miller,[†] Frank S. Modica,^{†,2} and Diek C. Koningsberger[‡]

^{*}Schuit Institute of Catalysis, Eindhoven University of Technology, P.O. Box 513, 5600 MB Eindhoven, The Netherlands; [†]AMOCO Research Center, P.O. Box 3011, Naperville, Illinois 60566-7011; and [‡]Debye Institute, Utrecht University, P.O. Box 80083, 3508 TB Utrecht, The Netherlands

Received September 22, 1995; revised April 26, 1996; accepted May 10, 1996

The relation between the catalytic activity, electronic properties, morphology, and structure of the metal-support interface was studied for Pt/ γ -Al₂O₃ after low (300°C, LTR) and high temperature reduction (450°C, HTR). EXAFS revealed that after LTR the platinum particles were three-dimensional, contained 11 Pt atoms on average, and were at a distance of 2.7 Å from the support oxygen. During HTR, the morphology of the platinum particles changed from three-dimensional to rafts with a structure similar to Pt(100), as indicated by a decrease in the Pt–Pt coordination number and the absence of the third coordination shell in the EXAFS spectrum. After HTR the Pt–O distance was shortened to 2.2 Å due to the desorption of hydrogen from the metal-support interface. The shortening of the Pt–O distance upon HTR treatment agrees with previous studies on zeolite supported platinum. However, zeolite supported platinum particles retained their three-dimensional structure upon HTR. The changes in the structure of the catalyst affected the catalytic, chemisorption, and electronic properties. After HTR the selectivity for hydrogenolysis of both neopentane and methylcyclopentane to methane decreased. At the same time the specific activity for neopentane isomerization and methylcyclopentane ring opening increased. The hydrogen chemisorption capacity after HTR was lower than after LTR. HTR shifted the asymmetric linear CO infrared absorption from 2063 to 2066 cm⁻¹. Comparison of the Pt L_{III} and L_{II} X-ray absorption edge intensities after LTR and HTR revealed that the number of holes in the *d*-band of the platinum atoms increased by 9.5% during HTR. It was suggested that the decrease in hydrogen chemisorption capacity, hydrogenolysis selectivity, and number of holes in the *d*-band are related to the change in the structure of the metal-support interface. The increase in specific activity for isomerization of neopentane and the shift in the CO infrared absorption band with a raise in reduction temperature agreed with reported

results for single crystals and was attributed to the higher concentration of atoms with Pt(100) symmetry in the catalyst after HTR.

© 1996 Academic Press, Inc.

INTRODUCTION

During the past decade many studies of the relation between the catalytic properties of supported metal catalysts and the reduction temperature have been published (1–6). Metal particles reduced at high temperatures (>500°C) supported on “reducible oxides” like titania show significant differences in catalytic behaviour in comparison to metal particles reduced at low temperature (1). Although the effects of high temperature reduction (HTR) are usually smaller for metals on “nonreducible” oxides, such as alumina or silica, differences in catalytic activity and selectivity for hydrogenolysis, isomerization, and aromatization reactions have been reported (2–6).

Several studies of platinum supported on nonreducible oxides have reported changes in the catalytic performance and the hydrogen chemisorption capacity after HTR; however, each study has attributed these changes to a different cause. Den Otter and Dautzenberg (2) and Menon and Froment (3) observed a drop in hydrogenolysis activity of a Pt/ γ -Al₂O₃ catalyst after reduction at temperatures higher than 550°C. In the former, the loss in activity was assumed to result from the formation of a Pt–Al alloy; while, in the latter study, the loss in activity after HTR was assigned to the presence of strongly chemisorbed hydrogen. Margitfalvi *et al.* (5) have shown that hydrogen treatment at 630°C of Pt/ γ -Al₂O₃ resulted in an increase in the aromatization selectivity in the dehydrocyclization of hexane and a decrease in hydrogenolysis selectivity. Similarly, reduction at 400°C of platinum films, vapour deposited on silica or alumina, resulted in a decrease in the turn over frequency (TOF) for the methylcyclopentane ring opening and decrease in the selectivity for *n*-hexane compared to reduction at low temperature (LTR, 275°C) (6). No hydrogenolysis was observed

¹ To whom correspondence should be addressed at present address: Mitsubishi Chemical Corporation, Yokohama Research Centre, 1000, Kamoshida-cho, Aoba-ku, Yokohama 227, Japan.

² Present Address: UOP Research Center, 50E Algonquin Rd., Des Plaines, IL 60017-5017, U.S.A.

in these experiments. Additionally, Abasov *et al.* (7) reported that the hydrogen chemisorption capacity of Pt/ γ -Al₂O₃ decreased from 0.51 to 0.08 upon hydrogen treatment at 700°C. The hydrogen chemisorption capacity could partially be restored by an oxidation–reduction treatment, suggesting a SMSI-like behaviour. Moreover, changes in the CO stretch frequency were observed. Decreases in hydrogenolysis activity and hydrogen chemisorption capacity have also been reported for platinum in acidic and neutral LTL zeolite (8–10). In these studies the structural characteristics of the catalysts were determined by EXAFS and H₂ TPD. It was concluded that after LTR a layer of atomic hydrogen resides between the platinum particle and the zeolite framework. During HTR, the interfacial hydrogen desorbs and platinum is left in direct contact with the oxide ions of the support. This change in the structure of the metal support interface was considered to be responsible for the observed changes in the catalytic and chemisorption properties of the metal.

This paper sets forth the above-described results for zeolite-supported platinum particles. To this end, the structural, electronic, and catalytic properties of a Pt/ γ -Al₂O₃ catalyst were studied after reduction at 300 and 450°C. The availability of information on the microstructure as well as on the catalytic and electronic properties allows comparison with results obtained for single crystals.

EXPERIMENTAL

Catalyst Preparation

A 1.0 wt% Pt/ γ -Al₂O₃ catalyst was prepared by pore volume impregnation of Ketjen CK-300 (200 m²/g, 0.6 cm³/g) with an aqueous solution of hexachloroplatinic acid (H₂PtCl₆). The catalyst was dried in air overnight at 120°C before it was reduced at 300°C (heating rate 3°/min) for 4 h. After reduction the catalyst was cooled to room temperature in flowing hydrogen, flushed with N₂, and exposed to air. Prior to use, the catalyst was dried *in situ* at 120°C for 2 h and reduced at either 300 or 450°C.

XAS Data Collection

X-ray absorption spectra were measured at the Synchrotron Radiation Source (SRS) in Daresbury, U.K., wiggler station 9.2, using a Si (220) double-crystal monochromator. The storage ring was operated with an electron energy of 2 GeV and a current between 120 and 250 mA. At the Pt L_{III} edge (11564 eV), the estimated resolution was 3 eV. The monochromator was detuned to 50% intensity to avoid the effects of higher harmonics present in the X-ray beam. The measurements were done in the transmission mode, using ion chambers filled with argon to absorb 20% of the X-ray beam in the first ion chamber and 80% of the X-ray beam in the second ion chamber. To decrease low-

and high-frequency noise as much as possible, each data point was counted for 1 s and 6 scans were averaged. The energies of the X-ray absorption spectra were calibrated separately at both the Pt L_{II} and L_{III} edge using the data of the platinum foil placed between the second and third ion chamber.

The sample was pressed into a self-supporting wafer (calculated to have an absorbance of 2.5) and placed in a controlled-atmosphere cell (11), with the sample handled in the absence of air. After drying in flowing helium at 120°C for 2 h the sample was heated at a rate of 5°/min to the reduction temperature in flowing deoxygenated and dried hydrogen at atmospheric pressure. The sample was held at the reduction temperature for 1 h and cooled to room temperature under flowing hydrogen. The X-ray absorption spectra were collected in a static hydrogen atmosphere, while the sample was cooled to –130°C with liquid nitrogen.

EXAFS Data Analysis

Standard methods were used to extract the EXAFS from the measured absorption and to analyse the spectra. Details can be found elsewhere (10, 12–14). Data for the phase shifts and backscattering amplitudes of the Pt–Pt and Pt–O absorber–scatterer pairs were obtained from EXAFS of Pt foil and Na₂Pt(OH)₆ respectively. These spectra have been published elsewhere (13, 15). Data ranges applied in the forward and inverse k^3 weighted Fourier transforms of the extraction process are listed in Table 1. Structural parameters of the model EXAFS were obtained by nonlinear least-squares refinement with analytical partial derivatives of the difference between the model EXAFS and the measured EXAFS (12). The values of the goodness of fit (ϵ_v^2) were calculated according to the prescription in the “Report on Standards and Criteria in XAFS Spectroscopy” (18). Standard deviations of the model parameters were calculated from the statistical error in the measured EXAFS, the difference between the model and measured EXAFS, and the correlations between the structural parameters of the model (14).

Temperature-Programmed Desorption

Temperature-programmed desorptions (TPD) were programmed at 5°/min to 50°C in flowing He. The He and H₂

TABLE 1
Crystallographic Data and Fourier Filtering Ranges
of Reference Compounds

Compound	Abs.–Sc. pair	FT range (Å ⁻¹)	FT ⁻¹ range (Å)	N	R (Å)	Ref.
Pt foil	Pt–Pt	2.16–20.41	1.39–3.09	12	2.774	(16)
Na ₂ Pt(OH) ₆	Pt–O	1.83–14.87	0.84–2.26	6	2.05	(17)

gases were purified by oxygen and 5 A molecular sieve traps. Desorbed gases were monitored with a Leybold quadrupole mass spectrometer.

Diffuse Reflectance Infrared Fourier Transform Spectroscopy (DRIFTS)

Samples were mounted in a DRIFTS cell connected to a gas system. After drying in flowing Ar at 120°C for 2 h the sample was reduced in flowing 10% H₂/Ar at either 300 or 450°C (heating rate 5°/min) for 1 h. Subsequently the sample was cooled in a static atmosphere of hydrogen to RT. The spectra were recorded with a Perkin-Elmer 1720X FT-IR spectrometer equipped with a DTGS detector, a diffuse reflectance accessory ('Collector' model, Barnes Analytic), and a standard controlled environmental chamber (Spectra-Tech, model 0030-103), and 256 spectra with a resolution of 4 cm⁻¹ were averaged. The reflectance from a typical catalyst sample relative to the open beam throughput, with the dome and (self-pressed) KBr windows in place, was about 2% *R* at 2000 cm⁻¹. The spectra are presented as diffuse absorbance ($-\log(R/R_0)$), analogous to absorbance used for transmission experiments (19). Spectral subtraction was performed on a Perkin-Elmer 3600 Data Station.

After collection of the data on the reduced sample, a CO flow was admitted to the sample at room temperature for 1 min. The cell was flushed with Ar to remove gaseous CO before collecting the spectra. The spectrum of the reduced sample was used as a background spectrum.

Hydrogen Chemisorption

The desorption isotherms of hydrogen were measured in a conventional volumetric glass apparatus. Hydrogen was purified by passage through oxygen and 5 A molecular sieve water traps. Typically, 0.5 g of catalyst was dried at 120°C prior to reduction. After reduction the catalyst was cooled in H₂ to 200°C and evacuated for 15 min. Subsequently, a known amount of hydrogen was admitted (activated adsorption). The sample was cooled to room temperature and the desorption isotherm was measured between 10 and 80 kPa. The H/Pt value was calculated by extrapolating the hydrogen desorption isotherm to zero pressure (20).

Catalytic Reactions

The conversion of neopentane or methylcyclopentane was measured at atmospheric pressure in a fixed-bed, bench-scale reactor at 300°C. The catalysts were prereduced at 300°C or 450°C and the conversion was adjusted to be between 2 and 10% by changing the space velocity. The composition of the reaction gas was 1.25 vol% neopentane or 4.35 vol% methylcyclopentane in H₂. The TOF was calculated using hydrogen chemisorption as a measure of the active platinum surface.

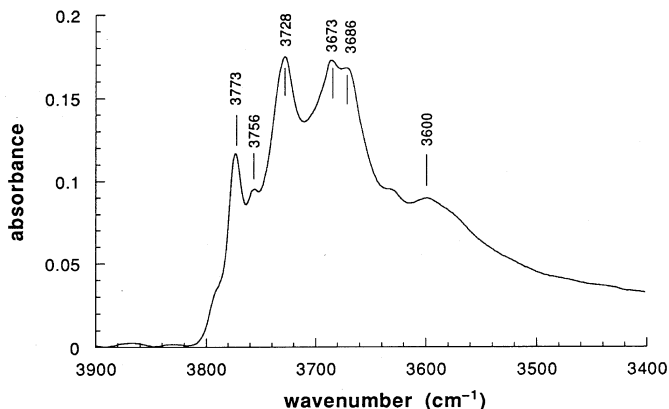


FIG. 1. Hydroxyl region of the infrared spectrum of γ -Al₂O₃ after heating in vacuum to 550°C.

RESULTS

Infrared Spectroscopy

The hydroxyl region of the infrared spectrum of bare γ -Al₂O₃ heated in vacuum to 550°C is shown in Fig. 1. At least 6 peaks can be distinguished (21). The DRIFT spectra of the Pt/ γ -Al₂O₃ after reduction at 300°C and 450°C are shown in Fig. 2. Only three peaks can be distinguished in the hydroxyl region. The peaks at 3730 and 3677 cm⁻¹ coincide with the peaks at 3728 and 3673 cm⁻¹ in the spectrum of bare γ -Al₂O₃, while the weak peak at 3600 cm⁻¹ increased in intensity and shifted to 3584 cm⁻¹. These results are consistent with those reported for Rh/ γ -Al₂O₃ (22). The features in the spectrum obtained after reduction at 450°C are similar to those in the spectrum obtained after reduction at 300°C. The difference spectrum (Fig. 2c) shows that the broad absorption below 3750 cm⁻¹ decreased in intensity. Moreover, the intensity of the peaks at 3584 and 3677 decreased while the peak at 3730 cm⁻¹ gained intensity. This might indicate

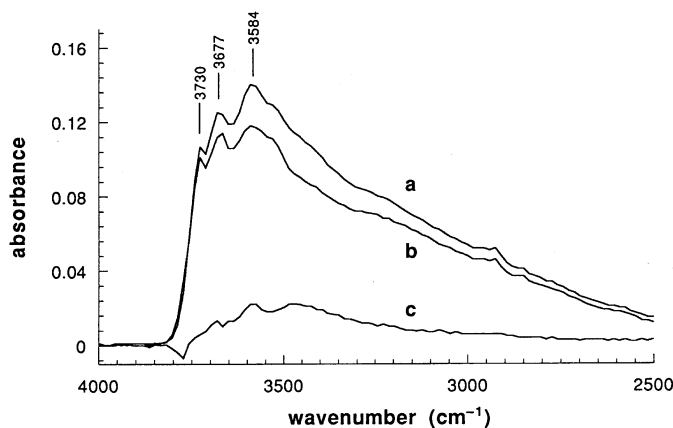


FIG. 2. Hydroxyl region of the infrared spectrum of Pt/ γ -Al₂O₃ after reduction at (a) 300°C and (b) 450°C, (c) being the difference between spectra a and b.

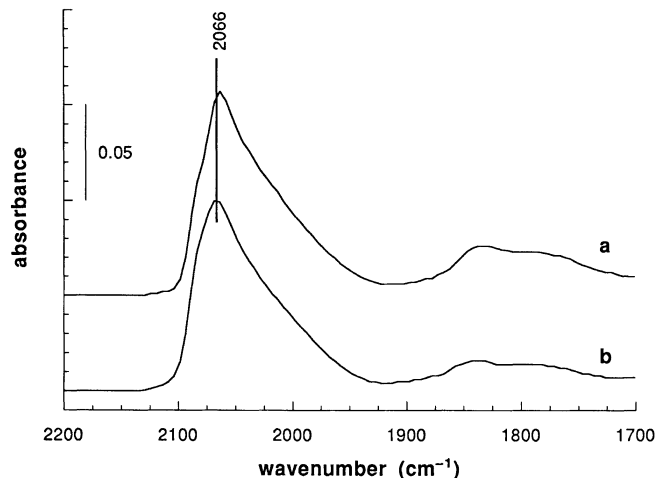


FIG. 3. Infrared spectrum of CO adsorbed on Pt/ γ -Al₂O₃ after reduction at (a) 300°C and (b) 450°C.

that the desorption of water diminished certain hydroxyl groups but created others (23).

DRIFT spectra obtained after adsorption of CO on the reduced Pt/ γ -Al₂O₃ catalyst are shown in Fig. 3. Both bridged and linear CO were present as indicated by the absorptions between 1750–1850 cm⁻¹ and 1950–2100 cm⁻¹, respectively. The absorption was lower after reduction at 450°C than after reduction at 300°C. Moreover, the maximum of the absorption peak shifted from 2063 cm⁻¹ to 2066 cm⁻¹ when the reduction temperature was raised from 300 to 450°C.

Temperature Programmed Desorption (TPD)

The desorption of water from the bare support heated to 300°C and the catalyst (after reduction at 300 and 450°C) is shown in Fig. 4a. The desorption of water started just above the reduction temperature. The amount of desorbed water was approximately equal for the support and for the catalyst reduced at 300°C. After reduction at 450°C only a small amount of water desorbed above 450°C.

In the hydrogen TPD of the catalyst reduced at 300°C (Fig. 4b), three peaks could be distinguished. The first peak with a maximum at 140°C has been attributed to chemisorbed hydrogen desorbing from the platinum particles (9). The broad desorption between 280 and 550°C was fitted with two gaussian peaks (Fig. 5): a large peak with a maximum at 435°C and a smaller one with a maximum at 325°C. The peak around 325°C has been assigned to the desorption of hydrogen from the metal-support interface (9, 10); hydrogen desorbing at higher temperatures has been suggested to originate from the support (9, 24).

After reduction at 450°C only a small amount of hydrogen desorbed below 200°C (Fig. 4b), indicating that the hydrogen chemisorption capacity of the catalyst decreased by reduction at 450°C. In addition, the peak around 325°C and

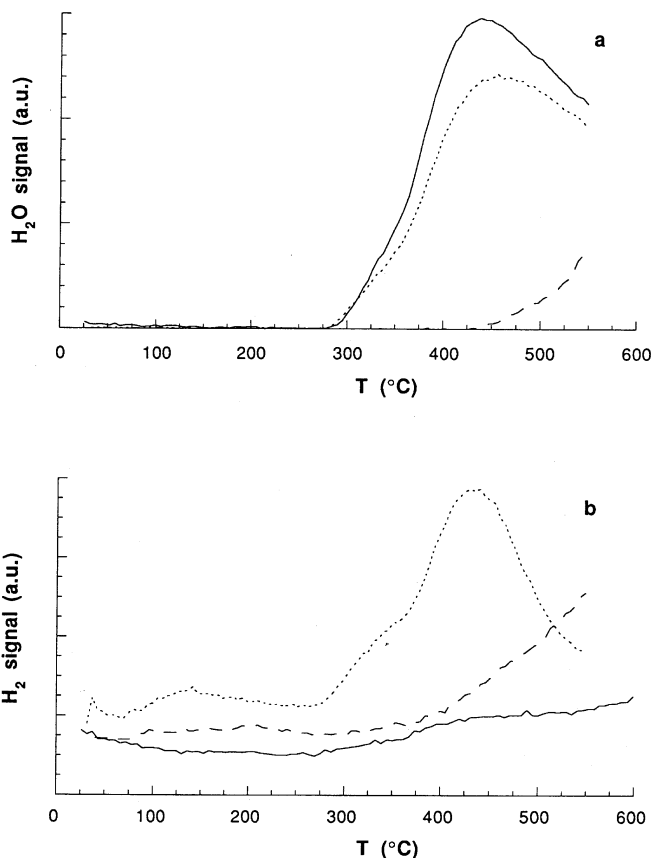


FIG. 4. TPD profile of bare γ -Al₂O₃ (solid line) and Pt/ γ -Al₂O₃ reduced at 300°C (dotted line) or 450°C (dashed line), (a) desorption of water and (b) desorption of hydrogen.

the large peak at 435°C were absent. Some hydrogen desorption occurred above 450°C.

EXAFS

EXAFS spectra obtained after reduction at 300 and 450°C are presented in Fig. 6. Data quality was high as

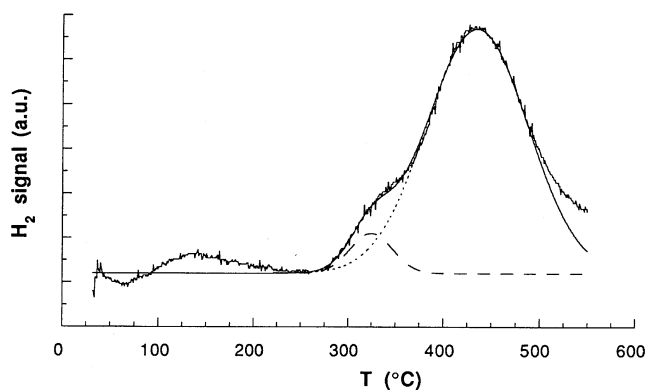


FIG. 5. Curve fitting result of the hydrogen TPD of Pt/ γ -Al₂O₃ reduced at 300°C.

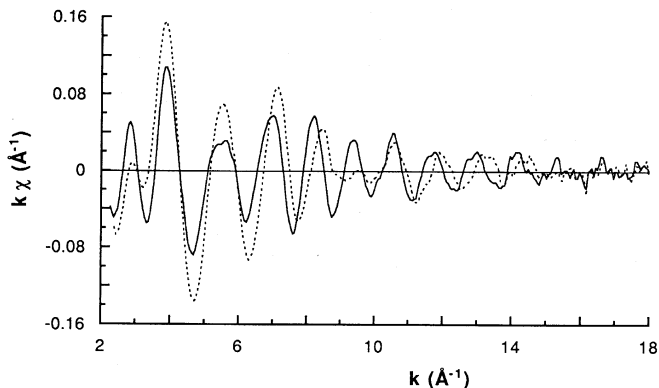


FIG. 6. EXAFS of Pt/ γ -Al₂O₃ after reduction at 300°C (solid line) and 450°C (dotted line).

indicated by the signal-to-noise ratios of 31 at 3.8 Å⁻¹ and 8 at 13.0 Å⁻¹ for the catalyst reduced at 300°C. The difference in nodes and the different envelopes of these EXAFS spectra indicate that the reduction temperature had a significant effect on the local structure around the platinum in Pt/ γ -Al₂O₃ catalysts. Normalised k^3 -weighted Pt–Pt phase- and amplitude-corrected Fourier transforms of these spectra are shown in Fig. 7 together with the Fourier transform of platinum foil. The Fourier transforms were normalized because the amplitude of the EXAFS (and hence of the Fourier transform) is much higher for the foil than for the catalyst. k^3 weighting was applied in order to emphasize the Pt–Pt contribution and to diminish the contribution of light elements, i.e., oxygen neighbours. The highest peak in the Fourier transform of the platinum foil was nearly perfectly symmetric due to the applied Pt–Pt phase correction (14, 15, 25). When the Fourier transform is not phase corrected the envelope of the Fourier transform of the Pt–Pt contribution is split into multiple peaks and the imaginary part of the Fourier transform is asymmetric because of the nonlinear k -dependence of the Pt–Pt phase shift and the k -dependent Pt backscattering amplitude. If the EXAFS of the Pt/ γ -Al₂O₃ would contain only Pt–Pt contributions it would also be symmetric. Hence, not only Pt–Pt contributions are present in the EXAFS of Pt/ γ -Al₂O₃.

The peak around 2.8 Å in the Fourier transform of the catalyst reduced at 300°C was located at a slightly shorter distance than the first shell Pt–Pt peak of Pt foil, Fig. 7a. Additionally, there was a small difference in the imaginary part of the Fourier transform in the region 2.2–2.4 Å. Higher shell peaks in the catalyst at the location of the second (3.92 Å) and third (4.80 Å) coordination shells of platinum foil were much smaller than those of the Pt foil, indicating small platinum particles in the catalyst. After reduction at 450°C the peak around 2.8 Å in the Fourier transform exhibited a large shift to shorter distance, Fig. 7b. Furthermore, an additional peak around 2.3 Å was visible. There were large differences in the imaginary part of the Fourier

transform of the catalyst and the foil, indicating that an additional scatterer was present. Higher shells in the catalyst reduced at 450°C were smaller than those of the catalyst reduced at 300°C. In addition, there was a small shift to shorter distance in the position of the nodes of the second Pt–Pt shell (3.92 Å) in the imaginary part of the Fourier transform. Furthermore, the third Pt–Pt shell (4.80 Å) was absent in the catalyst after reduction at 450°C.

The normalized k^1 -weighted Pt–Pt phase- and amplitude-corrected Fourier transforms of the catalysts after reduction at 300 and 450°C were compared with those of platinum foil in Fig. 8. In order to emphasize the contributions of oxygen atoms residing in the metal-support interface, the Fourier transform of the EXAFS spectrum was k^1 weighted. After reduction at 300°C the amplitude and imaginary part of the Fourier transform of the catalyst and platinum foil (Fig. 8a) were significantly different for distances ≤ 2.5 Å, indicating the presence of an additional scatterer. After reduction at 450°C (Fig. 8b) the differences were larger, showing that the magnitude of the additional contribution increased.

The first shell regions of the EXAFS spectra were separated from the remaining background and the higher shells

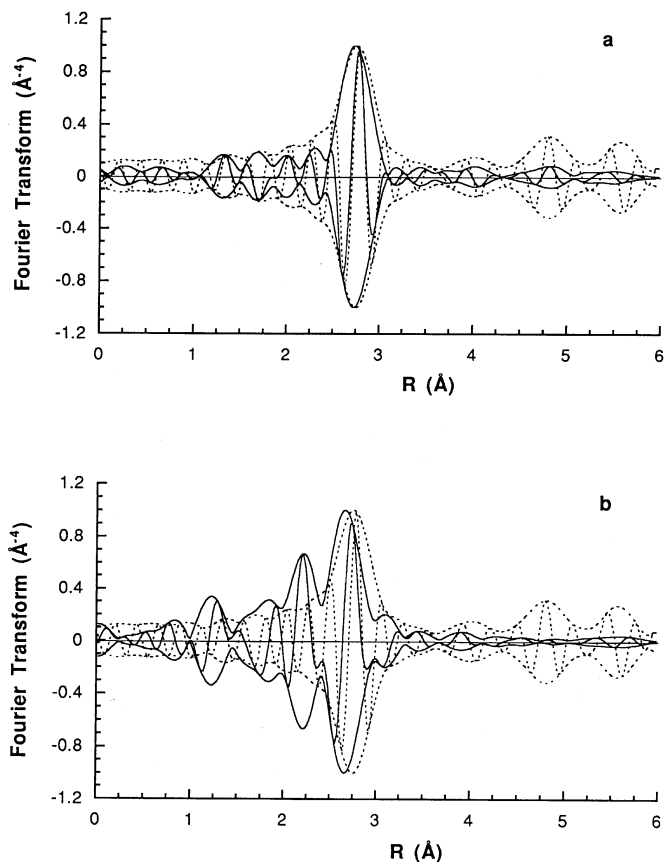


FIG. 7. Normalised Fourier transforms [k^3 , Δk : 3.1–13.1 Å⁻¹, Pt–Pt phase and amplitude corrected] of the EXAFS of (a) Pt/ γ -Al₂O₃ reduced at 300°C (solid line) and Pt foil (dotted line), (b) Pt/ γ -Al₂O₃ reduced at 450°C (solid line) and Pt foil (dotted line).

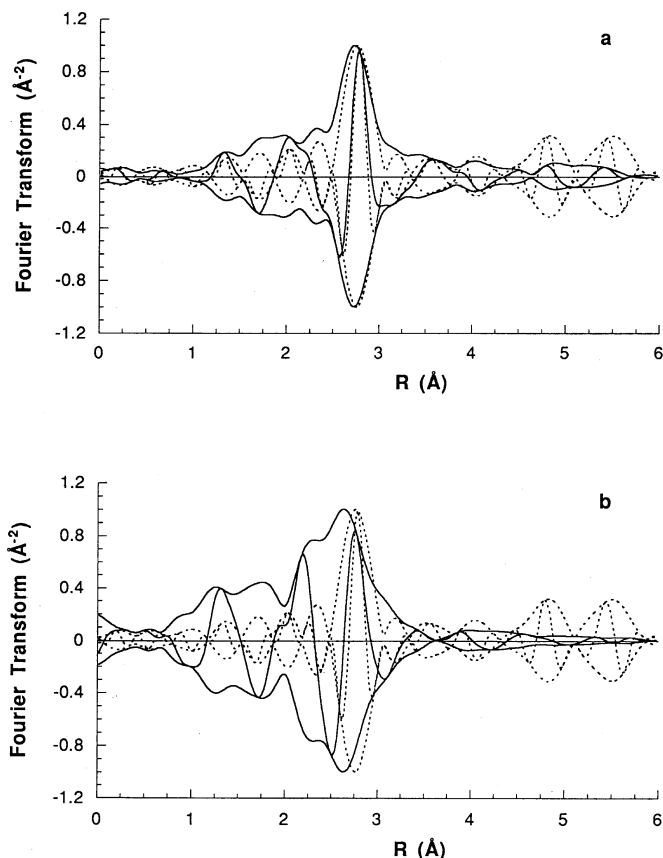


FIG. 8. Normalised Fourier transforms [k^1 , Δk : 3.1–13.1 \AA^{-1} , Pt–Pt phase and amplitude corrected] of the EXAFS of (a) Pt/ γ -Al₂O₃ reduced at 300°C (solid line) and Pt foil (dotted line), (b) Pt/ γ -Al₂O₃ reduced at 450°C (solid line) and Pt foil (dotted line).

by k^2 -weighted Fourier filtering. The Fourier filtering ranges (Δk and ΔR) are listed in Table 2. Table 2 also gives the analysis range (Δk) and the Goodness of Fit (ϵ_v^2) values (18).

The model EXAFS spectra calculated with the parameters in Table 3 are shown in Figs. 9a and 9b together with the Fourier-filtered EXAFS spectra. The agreement was very good. Figures 9c and 9d demonstrate that the Fourier transform of the model and the data were in good agreement as well.

After reduction at 300°C, the Pt–Pt distance of 2.76 \AA was identical to that of platinum foil. The Pt–Pt first-shell coordination number of 4.8 indicates that the platinum par-

TABLE 2

Fourier Filtering and Analysis Ranges and Goodness of Fit Values (ϵ_v^2)

T_{red} (°C)	FT range (\AA^{-1})	FT ⁻¹ range (\AA)	Analysis range (\AA^{-1})	ϵ_v^2
300	2.60–13.89	1.57–3.31	3.50–13.00	54.1
450	2.79–14.03	1.14–3.48	3.50–13.00	38.9

TABLE 3

Results of Refinement of Structural Parameters for EXAFS Spectra

T_{red} (°C)	Backscatterer	N	R (\AA)	$\Delta\sigma^2$ ($\times 10^{-3} \text{\AA}^{-2}$)	ΔE_0 (eV)
300	Pt	4.8 ± 0.1	2.76 ± 0.01	4.2 ± 0.1	2.1 ± 0.2
	O	1.2 ± 0.1	2.66 ± 0.01	7.0 ± 0.6	7.3 ± 0.4
450	Pt	3.8 ± 0.1	2.72 ± 0.01	5.5 ± 0.1	1.7 ± 0.2
	O	1.5 ± 0.1	2.25 ± 0.01	-2.3 ± 0.1	-13.5 ± 0.1

ticles are small. A coordination number of 4.8 corresponds to a spherical particle with 11 atoms. Reduction at 450°C brought about a first shell Pt–Pt distance of 2.72 \AA , 0.04 \AA shorter than after reduction at 300°C. Generally, platinum particles sinter during high-temperature reduction and the decrease in the first-shell Pt–Pt coordination number to 3.8 when the reduction temperature was raised to 450°C is therefore remarkable.

Contributions from oxygen atoms in the metal-support interface were present after reduction at both 300 and 450°C. After reduction at 300°C there was a Pt–O contribution at 2.66 \AA with a coordination number of 1.2. The distance of the Pt–O contribution after reduction at 450°C was 2.25 \AA , a decrease of 0.41 \AA . The shortening of the Pt–O distance with increasing reduction temperature is consistent with previous studies on a wide variety of noble metals and supports (10, 26). After reduction at 450°C the Pt–O coordination number was 1.5, a small increase compared to that of Pt/ γ -Al₂O₃ reduced at 300°C. In addition, there was a decrease in the Debye–Waller factor ($\Delta\sigma^2$) of the Pt–O contribution and an increase in the disorder of the Pt–Pt contribution when the reduction temperature was increased. This indicates that the distance distribution of the Pt–Pt contribution to the EXAFS becomes broader, while it becomes sharper for the Pt–O contribution, i.e., the distance between the platinum particle and the support.

Intensity of the Pt L_{III} and L_{II} X-Ray Absorption Edges

The intensity of both the Pt L_{III} and the Pt L_{II} X-ray absorption edges of the Pt/ γ -Al₂O₃ catalyst decreased with increasing reduction temperature (Fig. 10), but both were higher than the intensity of the corresponding edge of Pt foil. As the intensities of the Pt L_{III} and Pt L_{II} X-ray absorption edges are related to the number of holes in the d -band of the platinum metal, it is inferred that the platinum atoms in the catalyst had more holes in the d -band than did bulk platinum and that the number of holes decreased with increasing reduction temperature. Quantitative analysis of the difference in edge intensities with the method described by Mansour *et al.* (27) revealed that the fractional change in the number of holes in the d -band of the platinum particles was 9.5%, which converts to approximately 0.03 electrons/atom.

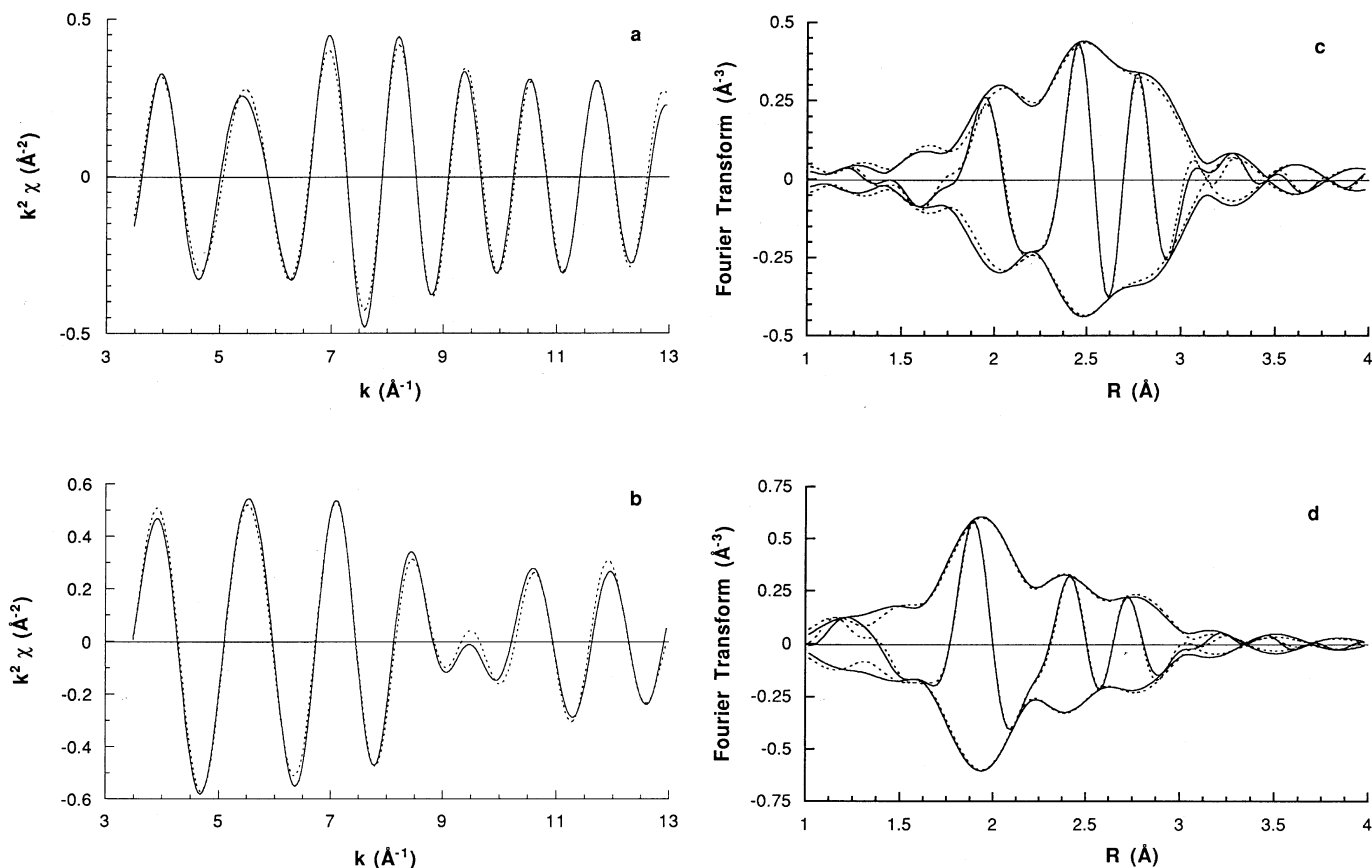


FIG. 9. Fit of Fourier filtered spectra (solid lines) and spectra calculated with the parameters in Table 3 (dotted lines): (a) k^2 -weighted EXAFS of Pt/ γ -Al₂O₃ reduced at 300°C; (b) k^2 weighted EXAFS of Pt/ γ -Al₂O₃ reduced at 450°C; (c) Fourier transform [k^2 weighted, Δk : 3.5–13.0 Å⁻¹] of the spectra shown in (a); (d) Fourier transform [k^2 weighted, Δk : 3.5–13.0 Å⁻¹] of the spectra shown in (b).

Hydrogen Chemisorption and Catalytic Reactions

The hydrogen chemisorption capacity, neopentane hydrogenolysis, and methylcyclopentane (MCP) ring opening TOFs are given in Table 4. Bare γ -Al₂O₃ did not convert any neopentane or MCP. For hydrogenolysis of neopentane, the TOF increased 2.3 times when the reduction temperature of Pt/ γ -Al₂O₃ was raised from 325 to 450°C. Simultaneously, the selectivity for neopentane hydrogenolysis (Table 5) decreased by 41%.

As shown in Table 4, the MCP ring opening TOF increased 2.6 times with increasing reduction temperature, which is equal within the limits of accuracy to the increase

in TOF observed for neopentane. The product selectivities for hydrogenolysis, ring opening, and aromatization are given in Table 6. As observed for hydrogenolysis of neopentane, the hydrogenolysis selectivity decreased when the reduction temperature was raised. The magnitude of the decrease (55%) was larger for MCP than for neopentane hydrogenolysis.

DISCUSSION

Infrared Spectroscopy and Temperature Programmed Desorption: The Surface of Alumina

The surface of γ -Al₂O₃ is covered with hydroxyl groups after reduction at 300°C. As the reduction temperature is

TABLE 4

Hydrogen Chemisorption (H/Pt) and TOF Values for Neopentane Hydrogenolysis and Methylcyclopentane Ring Opening

Reduction temperature (°C)	H/Pt	TOF neopentane (s ⁻¹)	TOF methylcyclopentane (s ⁻¹)
300	1.48	3.9×10^{-5}	1.2
450	1.18	9.1×10^{-5}	3.1

TABLE 5

Selectivity for the Conversion of Neopentane at Atmospheric Pressure ($T = 325^\circ\text{C}$, 1.25% Neopentane in H₂)

Reduction temperature (°C)	325	450
CH ₄	12.6	7.4
<i>i</i> -C ₄ H ₁₀	42.5	24.9
<i>i</i> -C ₅ H ₁₂	44.9	67.7

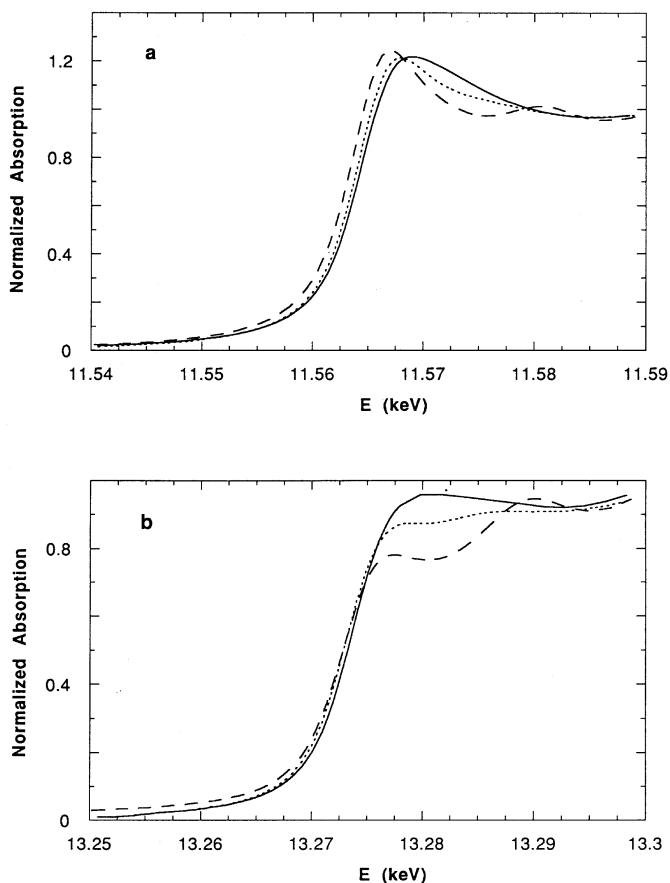


FIG. 10. Intensity of the X-ray absorption edge of Pt/ γ -Al₂O₃ reduced at 300°C (solid line) or 450°C (dotted line). The edges of Pt foil (dashed line) are shown for comparison: (a) Pt L_{III} edge, (b) Pt L_{II} edge.

increased, for example, to 450°C, there is a continuous decrease in the number of hydroxyl groups due to the progressive loss of water. Dehydroxylation of the support begins at temperatures above the reduction temperature.

The H₂ TPD indicates that there are three types of hydrogen on the catalyst after LTR. The 180°C desorption has previously been shown to correspond to chemisorbed hydrogen (9, 28). The quantity of hydrogen associated with the two remaining desorptions is approximately equal to

4 H/Pt. Therefore the TPD data suggest that the platinum may have been oxidized by water during the TPD to produce hydrogen and platinum (IV) oxide. However, there was no hydrogen consumption during a temperature-programmed reduction after the TPD. Similarly, infrared and EXAFS measurements of reduced Pt/H-LTL after H₂ TPD up to 600°C showed that the platinum remains metallic during the TPD (27). Hence, it is inferred that the platinum clusters are not oxidized during the TPD and that the evolved hydrogen originates from the support.

The H₂ TPD also indicates that reduction at 450°C results in changes of the alumina support. After HTR there is a loss of hydrogen that desorbs at high temperature. A similar loss of hydrogen that desorbs at high temperature was observed for zeolite (LTL and MAZ) supported platinum catalysts after HTR (9). The decrease in the amount of hydrogen that desorbs at high temperature coincides with the dehydroxylation of the support measured by DRIFTS and desorption of water. Hence, high temperature hydrogen desorptions appear to be associated with the presence of alumina hydroxyl groups (29).

EXAFS: The Structure of Platinum on Alumina

After reduction at 300°C, the average platinum particle contained 11 atoms ($N=4.8$). The Pt–Pt distance was 2.76 Å which is equivalent to that of platinum foil. After reduction at 450°C the Pt–Pt distance decreased to 2.72 Å, a decrease of 1.4%. Contraction of the nearest neighbour distance in platinum up to 4% has been reported for Pt/ γ -Al₂O₃ (28), Pt/H-FAU (30), and Pt/H-LTL (27) measured in the absence of chemisorbed hydrogen. Furthermore, it was shown that the platinum nearest neighbour distance relaxed to the bulk distance upon hydrogen chemisorption (28, 30). Hence, the decrease in the Pt–Pt distance upon reduction at 450°C is in agreement with the decrease in hydrogen chemisorption capacity (Table 4).

Reduction at 450°C lowered the Pt–Pt coordination number from 4.8 to 3.8. The decrease in the first-shell Pt–Pt coordination number indicates either a decrease in the platinum particle size due to a breakup of the particles during HTR or a change in the platinum particle morphology from three-dimensional to rafts. Fortunately, the EXAFS also supplied information on the morphology of the studied particles. The amplitude of the Fourier transform in the region of the second-shell (around 3.92 Å) did not change, while the third shell (around 4.80 Å) decreased significantly in amplitude (solid lines in Figs. 7a and 7b). Figure 11 shows which coordination shells are present in the surface layer of Pt(111) and Pt(100) crystals. In the (111) layer, which possesses sixfold symmetry, the second coordination shell is absent, while in the (100) layer, which possesses square symmetry, the third coordination shell is absent. Model calculations on the change in coordination number with the number of atoms in a raft or particle (Fig. 12) show that

TABLE 6

Selectivity for the Conversion of Methycyclopentane at Atmospheric Pressure ($T=300^\circ\text{C}$, 4.35% Methycyclopentane in H₂)

Reduction temperature (°C)	300	450
Methane	3.8	1.7
2-Methylpentane	62	66
3-Methylpentane	21	23
<i>n</i> -Hexane	13	9
Benzene	0.2	0.3

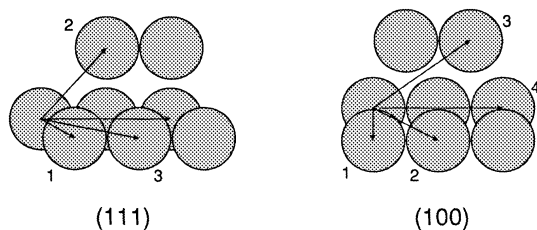


FIG. 11. The position of atoms that give rise to the coordination shells in the (111) and (100) planes of platinum.

platinum atoms in raft structures have a consistently lower first-shell coordination number than platinum atoms in a sphere. For the raft with (111) structure, the second-shell coordination number is always 0, and for the raft with (100) structure, the third-shell coordination number is always 0 (Fig. 11). Note also that the coordination numbers for the second and fourth shells of the raft with (100) structure are higher than for the three-dimensional particle with the same number of atoms. Combining the information on the change in coordination number and the Fourier transform

with the data on the different raft structures leaves little room for any other conclusion than that the platinum particles change morphology from three-dimensional to rafts with (100) structure. However, an 11 atom raft with (100) structure should exhibit a first-shell coordination number of 2.7, as opposed to the observed coordination number of 3.8. It is therefore likely that some sintering has taken place or that some three-dimensionality still remains. Finally, the Pt-O coordination number increased from 1.2 to 1.5 when the reduction temperature was raised from 300 to 450°C. This agrees very well with the flattening of the particle deduced from the Pt-Pt coordination number and hence more atoms in contact with the support.

The effect of reduction temperature on the structure of platinum particles supported on neutral and acidic zeolite LTL (10) differs from the results obtained for Pt/ γ -Al₂O₃. Platinum particles inside zeolite cavities sintered slightly with increasing reduction temperature but retained their three-dimensional structure. Although there are small differences between the platinum particles in the zeolite cavities and the platinum particles in the samples studied here,

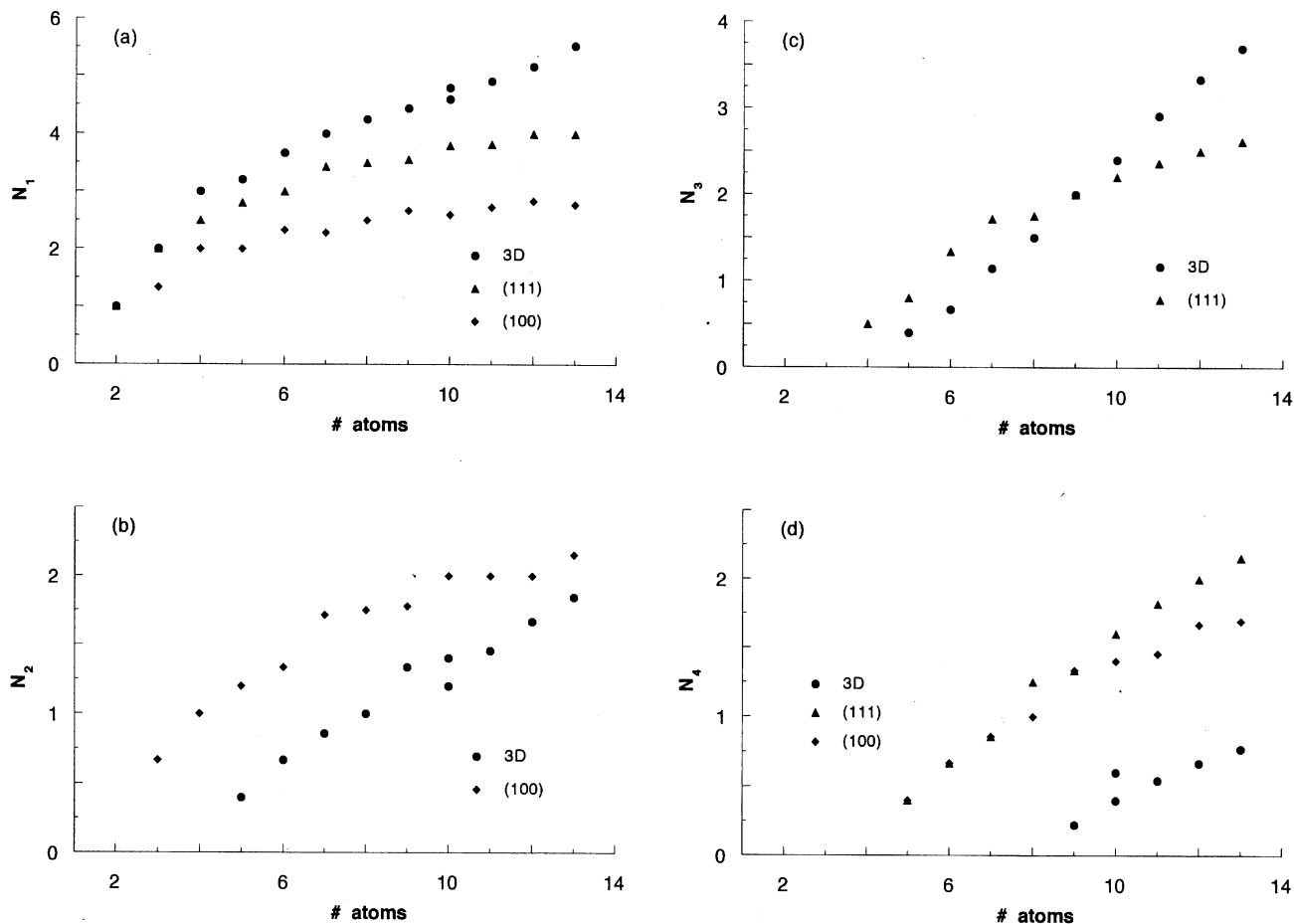


FIG. 12. Coordination number of the (a) first, (b) second, and (c) third shell as a function of the number of atoms. Atoms were added to the unoccupied position closest to the center of gravity of the particle.

the difference in particle morphology is likely due to the structure of the supports, i.e., γ -Al₂O₃ exposes a flat surface, while the cavities in zeolite LTL are circular.

After reduction at 300°C, the distance between the platinum atoms and the support oxygens is 2.66 Å which is longer than the radii of Pt (metallic, 1.39 Å) and O²⁻ (covalent, 0.73 Å). This is consistent with other studies on supported metal catalysts that were reduced at temperatures below 350°C (26). As the long Pt–O distance was also observed for Ir/MgO (31) and Pt/K-LTL (10), which both lack hydroxyl groups, the possibility that the long Pt–O distance is due to platinum on hydroxyl groups can be ruled out. This also implies that the shortening of the Pt–O distance is not related to the desorption of water observed in the TPD. Based on EXAFS and H₂ TPD analysis of Pt/K-LTL reduced at low temperature, it has been proposed that the long Pt–O distance originates from (neutral) hydrogen atoms located between the metal particles and the support (9, 10). The small hydrogen desorption observed at 325°C in the H₂ TPD most likely corresponds to loss of this interfacial hydrogen from Pt/ γ -Al₂O₃, bringing about the shortening of the Pt–O distance by 0.4 Å when the reduction temperature is raised from 300 to 450°C.

The increase in reduction temperature from 300 to 450°C was accompanied by a decrease in the disorder ($\Delta\sigma^2$) in the Pt–O coordination shell as well as in the edge energy shift (ΔE_0). These trends were previously reported for Pt/K-LTL and Pt/H-LTL (10) and the possibility of an alternative backscatterer was investigated. Since Pt/H-MAZ did not contain any residual potassium or sodium, but showed the same contributions to the EXAFS, it was concluded that oxygen was the scatterer in the contribution around 2.22 Å. Whether the surface of γ -Al₂O₃ contains Al³⁺ ions depends on the exposed crystal plane and layer (23). Therefore, there are no structural arguments to exclude a change in backscatterer. However, den Otter and Dautzenberg (2) reported that the formation of PtAl alloys did not take place below 550°C, which is 100°C higher than the reduction temperature used in this study. Finally, one can argue that the platinum will migrate over the surface to the Al³⁺ ions that have been uncovered by the desorption of water. Although this possibility cannot be ruled out, the agreement between the results obtained for zeolite-supported platinum particles and γ -Al₂O₃-supported platinum particles is considered enough evidence to conclude that support oxygen atoms are the actual backscatterers.

The disorder in the platinum particle increased, while the disorder in the Pt–O shell decreased upon the rise in reduction temperature. Hence, the interaction of the interfacial Pt atoms with the support becomes more uniform. The rather large decrease in ΔE_0 which accompanied the increase in reduction temperature may reflect the change in the properties of the interaction between Pt and O, but it cannot be ruled out that the desorption of interfacial hy-

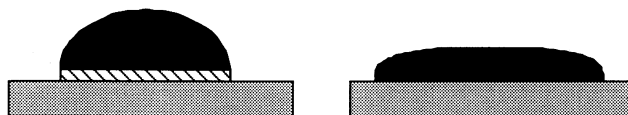


FIG. 13. Schematic representation of the structure of the platinum particles and the metal-support interface after reduction at 300°C (left) and 450°C (right).

drogen influences the phase shift of the oxygen atoms. The better uniformity of the Pt–O distances suggests that the platinum particles adapted to the epitaxy of the support. It would be worthwhile to prepare an atomic model of the interface structure, but the conflicting reports on the exposed crystal plane has prevented this. For example, electron microscopy (32) suggested the preferential exposure of the (111) plane, neutron diffraction (33) suggested the (100) and (110) plane, and low energy ion scattering (34) suggested that the D-layer of the (110) crystal plane is preferentially exposed. However, the spacing of the O atoms in Al₂O₃ is less than the spacing of the Pt atoms in bulk platinum, and an epitaxial adaption of the platinum to the alumina surface therefore requires a shortening of the Pt–Pt distance, as was actually observed.

A scheme of our understanding of the structure of metal particles supported by γ -Al₂O₃ and the metal-support interface is presented in Fig. 13. After reduction at 300°C the (hemi)spherical particles are separated from the alumina by a layer of hydrogen. This hydrogen evolves from the interface during treatment at high temperatures, bringing the platinum in direct contact with the oxygen atoms of the support and, in the case of alumina, changing the morphology of the platinum particle.

Electron Density: Infrared Spectroscopy and White Line Intensity

The shift to higher wavenumbers of the CO stretch frequency with increasing reduction temperature indicates that the electron density on the surface platinum atoms decreases with reduction temperature. In contrast, the number of holes in the *d*-band of the platinum atoms, as determined from the white line intensities, decreased when the reduction temperature is increased.

This apparent contradiction is straightforwardly explained when the results of the structure determination and the hydrogen chemisorption capacity are taken into account. First, the morphology of the platinum particles changed from three-dimensional to flat when the reduction temperature was raised, bringing about a lower number of nearest neighbours for the platinum atoms. This results in a decreased electron density and a shift to higher wavenumbers of the CO stretch frequency (35). Second, the white line intensity is in first approximation determined by the amount of chemisorbed hydrogen (28, 36, 37), i.e., more chemisorbed hydrogen results in higher white lines.

The hydrogen chemisorption measurements show that the amount of hydrogen chemisorbed per Pt atom decreases by $\approx 20\%$ when the reduction temperature was increased (Table 4). Moreover, interfacial hydrogen (present after reduction at 300°C , but absent after reduction at 450°C) is expected to increase the white line intensity too. Therefore, the observed decrease in white line intensity with increasing reduction temperature is attributed to the lower amount of chemisorbed hydrogen on the platinum particle and the absence of interfacial hydrogen, while the shift in CO stretch frequency is attributed to the change in morphology of the platinum particles. Despite the differences in origin of the effects, it is clear from both IR spectroscopy and the white line intensity that the electron density of the platinum atoms changed when the reduction temperature was raised.

The Influence of the Morphology of the Platinum Particles and the Structure of the Metal-Support Interface on Hydrogen Chemisorption Capacity and Catalytic Properties

Reduction of Pt/ γ - Al_2O_3 at 450°C resulted in dehydroxylation of the alumina, a flattening of the platinum particles, which was accompanied by a larger fraction of (100) facets being exposed, and the loss of hydrogen from the metal-support interface leaving the platinum in contact with the oxide surface. The hydrogen chemisorption capacity decreased with increasing reduction temperature. However, one would expect a higher hydrogen chemisorption capacity based on the lower Pt–Pt coordination number after HTR (38). A decrease in hydrogen chemisorption with increasing reduction temperature has also been observed for Pt/K-LTL and Pt/H-LTL catalysts (10). Furthermore, in these catalysts, HTR also resulted in a change in the structure of the metal-support interface due to the loss of interfacial hydrogen, but there was no evidence for a change in particle morphology after HTR. Therefore, it is likely that the change in the structure of the metal-support interface led to a change in the electronic state of platinum, which in turn suppressed the hydrogen chemisorption capacity.

The TOF for conversion of both MCP and neopentane increased by a factor of 2.5 with increasing reduction temperature. Changes in the activity of this magnitude may result from changes in the platinum particle size (39), the particle morphology (40), or from the intrinsic activity of the platinum atoms, i.e., the electronic properties. Regardless of which interpretation is correct, the observed changes in neopentane TOF are much smaller than the effects observed for changes in support acidity (9, 29, 41). For example, TOF for neopentane hydrogenolysis was higher by a factor of 10^5 \AA for Pt on acidic LTL compared to Pt on alkaline LTL (29). Additionally, increases in the neopentane TOF of about 10^2 have also been reported for Pt in acidic H-Y compared to Pt/ γ - Al_2O_3 (41), or about

10^2 for Pd in acidic H-Y compared to Pd/ SiO_2 (42). This suggests that the changes in the properties of the platinum due to higher reduction temperatures are qualitatively different from the effects induced by support acidity/basicity. Dehydroxylation of γ - Al_2O_3 changes the IR absorption frequency, i.e., the acidity of the surface hydroxyl groups. However, this will not affect the conversion of MCP or neopentane, as the bare support does not show activity under the reaction conditions.

While the TOF for both MCP and neopentane conversion increased with increasing reduction temperature, the isomerization and ring opening selectivity increased and the hydrogenolysis selectivity decreased (Tables 4–6). These changes in selectivity are consistent with other studies (43, 44). Although the hydrogenolysis selectivity decreased with increasing reduction temperature, the absolute TOFs for isomerization, ring opening, and hydrogenolysis increased, i.e., there is a larger increase in TOF for isomerization and ring opening than for hydrogenolysis after HTR. The EXAFS results showed that the platinum particles in the Pt/ γ - Al_2O_3 catalyst investigated here are three-dimensional after reduction at 300°C and flatten during reduction at 450°C . Moreover, the flattening is accompanied by a rearrangement that brings about an increase in the concentration of surface atoms with a symmetry similar to the Pt(100) surface. The higher isomerization TOF for the catalyst that possesses the same symmetry as Pt(100) agrees very well with single crystal studies on the skeletal rearrangements of small hydrocarbons over various Pt surfaces (45). Isomerization activity of Pt(100) is higher than isomerization activity of both the close packed Pt(111) surface and the kinked Pt(10, 8, 7) surface (45). Pt(10, 8, 7) has a very high concentration of kink sites and is hence more representative of a small metal particle than Pt(111). Therefore, it is inferred that the increased isomerization activity is related to the morphology change of the platinum particles.

As argued in the preceding paragraph, the specific hydrogenolysis activity of Pt/ γ - Al_2O_3 increased with reduction temperature. This can *not* be explained by the change in morphology, as single-crystal work (45) has shown that the hydrogenolysis activity of Pt(10, 8, 7) is higher than that of Pt(100). It is therefore proposed that the change in hydrogenolysis activity is related to the change in the structure of the metal-support interface and hence to the change in electron density distribution on the Pt atoms.

CONCLUSION

Differences in the structure, the electronic properties, and the activity for isomerization and hydrogenolysis of neopentane and methylcyclopentane of Pt/ γ - Al_2O_3 after reduction at 300 and 450°C were investigated with EXAFS, TPD, and diffuse reflectance IR spectroscopy. The alumina support was progressively dehydrated with

increasing reduction temperature. DRIFTS and TPD of H₂O showed that surface dehydroxylation started slightly above the reduction temperature. After LTR, large quantities of spillover hydrogen were present on the alumina. After HTR there was less spillover hydrogen which coincides with the loss of surface hydroxyl groups.

EXAFS revealed that the structure of the platinum particles as well as the structure of the metal-support interface changed when the reduction temperature was raised. The change in the structure of the metal-support interface agreed with studies of noble metal particles on other supports. After reduction at 300°C the particles were three-dimensional. An increase in the reduction temperature to 450°C brought about a flattening of the platinum particle and the rearrangement of the atoms in a structure similar to a Pt(100) surface. This change in morphology is unique to the Pt/ γ -Al₂O₃ catalyst.

The changes in the structure of the catalyst increased the frequency of the linear CO band and decreased the number of holes in the *d*-band. The increase in CO stretch frequency was related to the decreases in the number of nearest neighbours of the platinum particles, while the decrease in the number of holes in the *d*-band was suggested to originate from the lower hydrogen chemisorption capacity and the different structure of the metal-support interface.

The activity for hydrogenolysis of neopentane and methylcyclopentane increased less than the activity for isomerization of neopentane and ring opening of methylcyclopentane when the reduction temperature was raised. It was suggested that the increase in hydrogenolysis activity was related to the change in the structure of the metal-support interface. The increase in isomerization activity was attributed to the change in morphology by comparison with results for single crystals.

ACKNOWLEDGMENTS

The authors are indebted to Dr Menno J. Kappers for collecting the IR spectra. Joop van Grondelle assisted with the preparation of the catalyst. Dr Tijs Koerts' advice was invaluable for obtaining the TPD spectra. The Dutch Organisation for Scientific Research (NWO) provided travel funds to M.V. and D.C.K. and supplied beam time at the SRS.

REFERENCES

- Imelik, G., Naccache, C., Coudurier, G., Praliaud, H., Meriaudeau, P., Gallezot, P., Martin, G. A., and Vedrine, J. C., "Metal-Support and Metal-Additive Effects in Catalysis." Elsevier, Amsterdam, 1982.
- den Otter, G. J., and Dautzenberg, F. M., *J. Catal.* **53**, 116 (1978).
- Menon, P. G., and Froment, G. F., *Appl. Catal.* **1**, 31 (1981).
- Menon, P. G., and Froment, G. F., *J. Catal.* **59**, 138 (1979).
- Margitfalvi, J., Szedlacsek, P., Hegedüs, M., and Nagy, F., *Appl. Catal.* **15**, 69 (1985).
- Kramer, R., and Zuegg, H., *J. Catal.* **80**, 446 (1983).
- Abasov, S. I., Borovkov, V. Y., and Kazansky, V. B., *Catal. Lett.* **15**, 269 (1992).
- Vaarkamp, M., van Grondelle, J., van Santen, R. A., Miller, J. T., Modica, F. S., Lane, G. S., and Koningsberger, D. C., in "Proc. 9th Int. Zeolite Conf., Montreal, 1992" (R. von Ballmoos, J. B. Higgins, and M. M. J. Treacy, Eds.), p. 443. Butterworth-Heinemann, London, 1993.
- Miller, J. T., Meyers, B. M., Modica, F. S., Vaarkamp, M., and Koningsberger, D. C., *J. Catal.* **143**, 395 (1993).
- Vaarkamp, M., Modica, F. S., Miller, J. T., and Koningsberger, D. C., *J. Catal.* **144**, 611 (1993).
- Kampers, F. W. H., Maas, T. M. J., van Grondelle, J., Brinkgreve, P., and Koningsberger, D. C., *Rev. Sci. Instrum.* **60**, 2635 (1989).
- Vaarkamp, M., Linders, J. C., and Koningsberger, D. C., in "Proc. XAFS VIII, Berlin, 1994," *Physica B* **208/209**, 159 (1995).
- Vaarkamp, M., Dring, I., Oldman, R. J., Stern, E. A., and Koningsberger, D. C., *Phys. Rev. B* **50**, 7872 (1994).
- Vaarkamp, M. Ph.D. thesis Eindhoven University of Technology, Eindhoven, 1993.
- Kampers, F. W. H., Ph.D. thesis Eindhoven University of Technology, Eindhoven, 1989.
- Wyckoff, W. G., "Crystal Structures." Interscience, New York, 1974.
- Trömel, M., and Lupprich, E., *Z. Anorg. Chem.* **414**, 160 (1975).
- Lytle, F. W., Sayers, D. E., and Stern, E. A., *Physica B* **158**, 701 (1988).
- Smyrl, N. R., Fuller, E. L., and Powell, G. L., *Appl. Spectrosc.* **37**, 38 (1983).
- Benson, J. E., and Boudart, M., *J. Catal.* **4**, 704 (1965).
- Okamoto, Y., and Imanaka, T., *J. Phys. Chem.* **92**, 7102 (1988).
- Cavanagh, R. R., and Yates, J. T., Jr., *J. Catal.* **68**, 22 (1981).
- Knözinger, H., and Ratnasamy, P., *Catal. Rev.-Sci.Eng.* **17**, 31 (1978).
- Miller, J. T., Meyers, B. L., Barr, M. K., Modica, F. S., and Koningsberger, D. C., *J. Catal.* **159**, 41 (1996).
- van Zon, J. B. A. D., Koningsberger, D. C., van't Blik, H. F. J., and Sayers, D. E., *J. Chem. Phys.* **82**, 5742 (1985).
- Koningsberger, D. C., and Gates, B. C., *Catal. Lett.* **14**, 271 (1992).
- Vaarkamp, M., Mojet, B. L., Kappers, M. J., Miller, J. T., and Koningsberger, D. C., *J. Phys. Chem.* **99**, 16067 (1995).
- Vaarkamp, M., and Koningsberger, D. C., submitted for publication.
- Modica, F. S., Miller, J. T., Meyers, B. L., and Koningsberger, D. C., *Catal. Today* **21**, 37 (1994).
- Moraweck, B., Clugnet, G., and Renouprez, A. J., *Surf. Sci.* **81**, L631 (1979).
- van Zon, F. B. M., Maloney, S. D., Gates, B. C., and Koningsberger, D. C., *J. Phys. Chem.* **115**, 10317 (1993).
- Iijima, S., *Surf. Sci.* **156**, 1003 (1985).
- Beaufils, J. P., and Barbaux, Y., *J. Chim. Phys.* **78**, 347 (1981).
- Stobbe-Kreemers, A. W., van Leerdam, G. C., Jacobs, J. -, Brongersma, H. H., and Scholten, J. J. F., *J. Catal.* **152**, 130 (1995).
- Kappers, M. J., and van der Maas, J. H., *Catal. Lett.* **10**, 365 (1991).
- Lytle, F. W., Greeger, R. B., Marques, E. C., Biebesheimer, V. A., Sandstorm, D. R., Horsley, J. A., Via, G. H., and Sinfelt, J. H., *ACS Symp. Ser.* **288**, 280 (1985).
- Vaarkamp, M., Miller, J. T., Modica, F. S., and Koningsberger, D. C., in "Proc. XAFS VII, Kobe, 1994," *Jpn. J. Appl. Phys.* **32 Suppl.** **32-2** 454 (1993)
- Kip, B. J., Duivenvoorden, F. B. M., Koningsberger, D. C., and Prins, R., *J. Am. Chem. Soc.* **108**, 5633 (1986).
- Che, M., and Bennett, C. O., *Adv. Catal.* **36**, 55 (1989).
- Gillespie, W. D., Herz, R. K., Petersen, E. E., and Somorjai, G. A., *J. Catal.* **70**, 147 (1981).
- Boudart, M., and Dalla Betta, R. A., in "Proc. 5th International Congress on Catalysis, Palm Beach, 1972" (J. H. Hightower, Ed.), p. 1329. North-Holland, Amsterdam, 1973.
- Homeyer, S. T., Karpinski, Z., and Sachtler, W. M. H., *J. Catal.* **123**, 60 (1990).
- Gault, F. G., *Adv. Catal.* **30**, 1 (1981).
- Anderson, J. B. F., Burch, R., and Cairns, J. A., *J. Catal.* **107**, 351 (1987).
- Davis, S. M., Zaera, F., and Somorjai, G. A., *J. Am. Chem. Soc.* **104**, 7453 (1982).